



Variability and trends in the global tropopause estimated from radiosonde data

Dian J. Seidel¹ and William J. Randel²

Received 3 April 2006; revised 3 July 2006; accepted 18 July 2006; published 3 November 2006.

[1] This study examines global tropopause variability on synoptic, monthly, seasonal, and multidecadal timescales using 1980–2004 radiosonde data. On synoptic and monthly timescales, tropopause height variations are anticorrelated with stratospheric temperature variations and positively correlated with tropospheric temperature variations. Correlations are stronger in the extratropics than in the tropics, for the upper troposphere (500–300 hPa) than for the lower troposphere, and for the lower stratosphere than for the middle stratosphere. The extratropical tropopause is more sensitive to temperature changes than the tropical tropopause, and in both regions, monthly anomalies of tropopause height are more sensitive to stratospheric temperature change than tropospheric, rising 2–3 km per degree cooling of the lower stratosphere. Tropopause height trends over 1980–2004 are upward at almost all of the (predominantly extratropical) stations analyzed, yielding an estimated global trend of 64 ± 21 m/decade, a corresponding tropopause pressure trend of -1.7 ± 0.6 hPa/decade, and tropopause temperature decrease of 0.41 ± 0.09 K/decade. These tropopause trends are accompanied by significant stratospheric cooling and smaller tropospheric warming. However, the tropopause trends are spatially correlated with stratospheric temperature trends and uncorrelated with tropospheric temperature trends. This association of tropopause height and stratospheric temperature trends, together with the presence of a significant quasi-biennial oscillation signal in tropopause height, suggests that at these lowest frequencies the tropopause is primarily coupled with stratospheric temperatures. Therefore, as an indicator of climate change, long-term changes in the tropopause may carry less information about changes throughout the vertical temperature profile than has been suggested by previous studies using reanalyses and global climate models.

Citation: Seidel, D. J., and W. J. Randel (2006), Variability and trends in the global tropopause estimated from radiosonde data, *J. Geophys. Res.*, *111*, D21101, doi:10.1029/2006JD007363.

1. Introduction

[2] Recent work by *Sausen and Santer* [2003] and *Santer et al.* [2003a, 2003b, 2004] suggests that changes in the height (or pressure) of the global tropopause may be a sensitive indicator of anthropogenic climate change. These studies employed reanalysis data and climate model simulations, in which tropopause height increases were closely associated with tropospheric warming and stratospheric cooling. Global tropopause pressure changes in the ECMWF 15-year reanalysis for 1979–1993 have been estimated between +0.1 and -1.13 hPa/decade [*Hoinka*, 1998, 1999; *Santer et al.*, 2003a], and the ECMWF 40-year reanalysis and the NCEP/NCAR reanalysis both show larger trends of about -2 hPa/decade for 1979–2001 [*Santer et al.*, 2003a, 2004]. These reported tropopause trends in reanalyses are remarkable given that typical reanalysis vertical resolution is about 50 hPa in the vicinity

of the tropopause, and that the tropopause is calculated by interpolation of lapse rates between model or analysis levels. To date, no studies have reported global tropopause trends based on the primary upper air data source entering the reanalyses—radiosonde data, although several investigators have done so for limited regions [*Nagurny*, 1998; *Highwood et al.*, 2000; *Randel et al.*, 2000; *Chakrabarty et al.*, 2000; *Seidel et al.*, 2001; *Varotsos et al.*, 2004; *Añel et al.*, 2006].

[3] In this study, we attempt to estimate trends in the global tropopause on the basis of radiosonde observations, which offer substantially higher vertical resolution than reanalyses, thus allowing a more accurate identification of the tropopause and possible multiple tropopause levels. Daily or twice-daily soundings, extending back about 50 years at some locations, present the possibility of examining tropopause variations on timescales ranging from synoptic to multidecadal. To provide a broader context for the analysis of long-term tropopause changes, we also examine the covariability of tropopause height and stratospheric and tropospheric temperature.

[4] Section 2 outlines the radiosonde data used and methods of analysis, including a discussion of temporal

¹NOAA Air Resources Laboratory, Silver Spring, Maryland, USA.

²National Center for Atmospheric Research, Boulder, Colorado, USA.

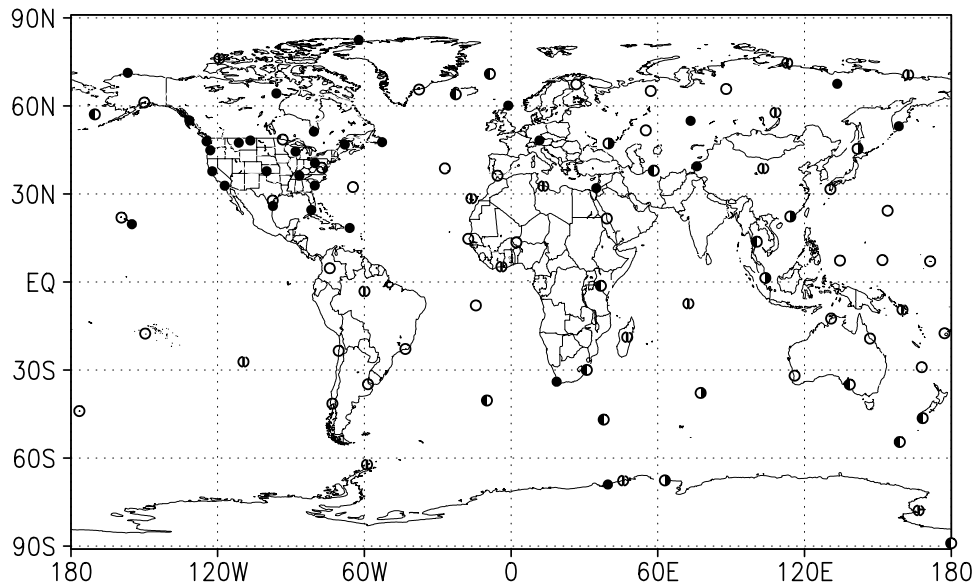


Figure 1. Locations of radiosonde stations used in this study. Solid circles indicate that data for both 0000 and 1200 UTC were used. Half-solid circles indicate that data for only one observation time were used; if 0000 (1200) UTC data were used, the left (right) side of the circle is solid. Open circles indicate that no data were used, and circles with a vertical line in the center indicate that data were used only in the creation of climatological means and zonal time series.

inhomogeneity in the observations. Section 3 discusses the climatological location and temperature of the tropopause and its mean seasonal cycle. Section 4 compares the typical magnitudes of tropopause height and pressure variability on different timescales, and section 5 discusses the day-to-day and monthly covariability of tropopause height and the temperature profile. Trends in tropopause height, pressure and temperature are presented in section 6, and a summary is given in section 7. Appendix A discusses the effect of reducing the vertical resolution of sounding data on our results.

2. Data and Methods

2.1. Radiosonde Observations

[5] Our analysis is based on radiosonde observations from the 100 stations shown in Figure 1 and listed in Table 1 obtained from the Integrated Global Radiosonde Archive [Durre *et al.*, 2006] at the NOAA National Climatic Data Center (NCDC). These stations were selected on the basis of the length and completeness of their archived data record, with an aim toward global coverage. Many of the stations have been extensively studied by Gaffen [1994], Lanzante *et al.* [2003], Free *et al.* [2005], and Randel and Wu [2006] and so some of their station histories and idiosyncrasies were familiar to us.

[6] Using all available soundings taken during the period 1958–2004 and within three hours of 0000 or 1200 UTC, we determined the location of the lapse rate tropopause (LRT, or LRT1) and, if present, the second tropopause (LRT2), using the definition promulgated by the World Meteorological Organization’s Commission for Aerology [World Meteorological Organization, 1957, p. 137], which we cite here because the original reference is not readily available:

(a) The first tropopause is defined as the lowest level at which the lapse rate decreases to $2^{\circ}\text{C}/\text{km}$ or less, provided also the average lapse rate between this level and all higher levels within 2 km does not exceed $2^{\circ}\text{C}/\text{km}$.

(b) If above the first tropopause the average lapse rate between any level and all higher levels within 1 km exceeds $3^{\circ}\text{C}/\text{km}$, then a second tropopause is defined by the same criterion as under (a). This tropopause may be either within or above the 1 km layer.

[7] We used all reported levels of data (both the standard and “significant” levels) but did not rely on the reported LRT in the sounding data, because these values are sometimes unreliable and often missing (J. C. Antuña *et al.*, Impact of missing sounding reports on mandatory levels and tropopause statistics: A case study, unpublished manuscript, 2006). (Appendix A examines the influence of reducing the vertical resolution of the soundings by ignoring significant level data on our results.) In addition to identifying the pressure, temperature, and geopotential height (interpolating the existing height data when necessary) of the tropopause(s), we also extracted temperature and height data for the surface and the 850, 500, 300, 200, 150, 100, 70, 50, 30, 20 hPa levels, and computed the layer mean temperature for 850–300 hPa and 100–50 hPa. Soundings with no identifiable LRT or with scanty data were not included. A companion paper, in preparation, focuses on the definition and characteristics of the second tropopause, which is often evident in the extratropics. Here our main interest is in the first tropopause and its relation to the temperature profile above and below it.

[8] The daily soundings were used to create time series for analysis of variability on four timescales: synoptic, monthly, seasonal, and multidecadal, separately for the two observation times. The mean seasonal cycle was computed by averaging all soundings for each calendar

Table 1. Radiosonde Stations Used in This Study, Including Latitude, Longitude, World Meteorological Organization Identification Number, and an Indication of What Data Were Used

| Station | Latitude | Longitude ^a | ID | Data ^b |
|---------------------|----------|------------------------|-------|-------------------|
| Alert | 82.50 | -62.33 | 71082 | 5 |
| Mould Bay | 76.23 | -119.33 | 71072 | 2 |
| Preobrazheniya | 74.67 | 112.93 | 21504 | 2 |
| Point Barrow | 71.30 | -156.78 | 70026 | 5 |
| Jan Mayen | 70.93 | -8.67 | 01001 | 3 R |
| Chetyrekhtolbovoy | 70.63 | 162.40 | 21965 | 2 |
| Verkhoyansk | 67.55 | 133.38 | 24266 | 5 |
| Sodankyla | 67.37 | 26.65 | 02836 | 1 R |
| Turuhsansk | 65.78 | 87.95 | 23472 | 1 L |
| Angmagssalik | 65.60 | -37.63 | 04360 | 1 R |
| Pechora | 65.12 | 57.10 | 23418 | 1 L |
| Baker Lake | 64.30 | -96.00 | 71926 | 5 |
| Keflavik | 63.97 | -22.60 | 04018 | 3 L |
| Anchorage | 61.16 | -149.98 | 70273 | 1 S |
| Lerwick | 60.13 | -1.18 | 03005 | 5 |
| Kirensk | 57.77 | 108.12 | 30230 | 2 |
| Saint Paul Island | 57.15 | -170.22 | 70308 | 3 R |
| Annette Island | 55.03 | -131.57 | 70398 | 5 |
| Omsk | 54.93 | 73.40 | 28698 | 5 |
| Petrovsk | 53.08 | 158.55 | 32540 | 5 |
| Orenburg | 51.68 | 55.10 | 35121 | 1 L |
| Moosonee | 51.27 | -80.65 | 71836 | 5 |
| International Falls | 48.57 | -93.38 | 72747 | 1 S |
| Munich | 48.25 | 11.58 | 10868 | 5 |
| Glasgow | 48.21 | -106.63 | 72768 | 5 |
| Quillayute | 47.95 | -124.55 | 72797 | 5 |
| Torbay | 47.67 | -52.75 | 71801 | 5 |
| Great Falls | 47.48 | -111.35 | 72776 | 5 |
| Rostov-on-Donu | 47.25 | 39.82 | 34731 | 4 L |
| Caribou | 46.87 | -68.02 | 72712 | 5 |
| Wakkanai | 45.42 | 141.68 | 47401 | 4 L |
| Salem | 44.92 | -123.02 | 72694 | 5 |
| Green Bay | 44.48 | -88.13 | 72645 | 5 |
| Pittsburgh | 40.53 | -80.23 | 72520 | 5 |
| Kashi | 39.47 | 75.98 | 51709 | 5 |
| Sterling | 38.98 | -77.48 | 72403 | 1 S |
| Lajes | 38.73 | -27.07 | 08508 | 1 LV |
| Minqin | 38.72 | 103.10 | 52681 | 2 |
| Ashabad | 37.97 | 58.33 | 38880 | 3 |
| Dodge City | 37.77 | -99.97 | 72451 | 5 |
| Oakland | 37.75 | -122.22 | 72493 | 5 |
| Nashville | 36.25 | -86.57 | 72327 | 5 |
| North Front | 36.25 | -5.55 | 08495 | 1 L |
| Charleston | 32.90 | -80.30 | 72208 | 5 |
| Miramar | 32.85 | -117.12 | 72293 | 5 |
| Tripoli | 32.68 | 13.17 | 62010 | 2 LV |
| Bermuda | 32.37 | -64.68 | 78016 | 1 LR |
| Bet Dagan | 32.00 | 34.82 | 40179 | 5 |
| Kagoshima | 31.63 | 130.60 | 47827 | 1 L |
| Santa Cruz | 28.47 | -16.25 | 60020 | 2 R |
| Corpus Christi | 27.78 | -97.51 | 72251 | 1 SV |
| Brownsville | 25.92 | -97.42 | 72250 | 5 |
| Key West | 24.58 | -81.70 | 72201 | 5 |
| Minamitorishima | 24.30 | 153.97 | 47991 | 1 LV |
| Hong Kong | 22.32 | 114.17 | 45004 | 4 R |
| Lihue | 21.98 | -159.35 | 91165 | 1 S |
| Jeddah | 21.67 | 39.15 | 41024 | 1 L |
| Hilo | 19.72 | -155.07 | 91285 | 5 |
| San Juan | 18.43 | -66.00 | 78526 | 5 |
| Dakar | 14.73 | -17.50 | 61641 | 1 LR |
| Bangkok | 13.73 | 100.50 | 48455 | 3 |
| Niamey | 13.48 | 2.17 | 61052 | 1 V |
| Truk | 7.47 | 151.85 | 91334 | 1 LS |
| Koror | 7.33 | 134.48 | 91408 | 1 LV |
| Majuro | 7.08 | 171.38 | 91376 | 1 R |
| Abidjan | 5.25 | -3.93 | 65578 | 2 |
| Bogota | 4.70 | -74.15 | 80222 | 1 R |
| Singapore | 1.37 | 103.98 | 48698 | 4 R |
| Nairobi | -1.30 | 36.75 | 63741 | 3 |
| Manaus | -3.15 | -59.98 | 82332 | 2 |
| Diego Garcia | -7.35 | 72.48 | 61967 | 2 |

Table 1. (continued)

| Station | Latitude | Longitude ^a | ID | Data ^b |
|------------------|----------|------------------------|-------|-------------------|
| Ascension Island | -7.97 | -14.40 | 61902 | 1 R |
| Honiara | -9.42 | 160.05 | 91517 | 2 |
| Darwin | -12.43 | 130.87 | 94120 | 1 LV |
| Nandi | -17.45 | 177.27 | 91680 | 1 R |
| Papeete | -17.55 | -149.62 | 91938 | 1 R |
| Antananarivo | -18.80 | 47.48 | 67083 | 2 |
| Townsville | -19.25 | 146.77 | 94294 | 1 L |
| Rio de Janeiro | -22.82 | -43.25 | 83746 | 1 V |
| Antofagasta | -23.42 | -70.47 | 85442 | 1 R |
| Isla de Pascua | -27.17 | -109.43 | 85469 | 2 |
| Norfolk Island | -29.03 | 167.93 | 94996 | 1 LV |
| Durban | -29.97 | 30.95 | 68588 | 3 V |
| Perth | -31.92 | 115.97 | 94610 | 1 LRV |
| Capetown | -33.96 | 18.60 | 68816 | 5 |
| Buenos Aires | -34.82 | -58.53 | 87576 | 1 R |
| Adelaide | -34.95 | 138.53 | 94672 | 3 L |
| Martin de Vivies | -37.80 | 77.53 | 61996 | 4 |
| Gough Island | -40.35 | -9.88 | 68906 | 3 L |
| Puerto Montt | -41.43 | -73.10 | 85799 | 1 R |
| Chatham Island | -43.95 | -176.57 | 93986 | 1 R |
| Invercargill | -46.40 | 168.33 | 93844 | 3 L |
| Marion Island | -46.88 | 37.87 | 68994 | 3 L |
| Macquarie Island | -54.50 | 158.95 | 94998 | 3 L |
| Bellingshausen | -62.20 | -58.93 | 89050 | 2 |
| Syowa | -69.00 | 39.58 | 89532 | 5 |
| Mawson | -67.60 | 62.88 | 89564 | 4 |
| Molodezhnaya | -67.67 | 45.85 | 89542 | 2 |
| McMurdo | -77.85 | 166.67 | 89664 | 2 R |
| Amundsen Scott | -90.00 | 180.00 | 89009 | 3 |

^aPositive, east; negative, west.

^bData indicators are as follows: 1, no data were used because of suspected inhomogeneities (except in Figure 8 (left)); 2, data were not used because of insufficient sampling, except to create climatological stations means and zonal-average time series and trends; 3, only 0000 UTC data were used; 4, only 1200 UTC data were used; 5, 0000 and 1200 UTC data were used. The reason for suspecting that data from stations with data indicators 1, 3, or 4 may be temporally inhomogeneous during the period 1980–2004 (for one or both observation times) is indicated by the codes L (change points identified by *Lanzante et al.* [2003]), R (satellite-radiosonde comparison by *Randel and Wu* [2006]), S (station history information, including *Gaffen* [1993] and *Elliott et al.* [2002]), and/or V (visual inspection of tropopause height anomaly time series).

month. Monthly means for each month were calculated if at least 50% of the expected observations were available. Monthly anomaly time series were computed by subtracting the mean seasonal cycle from the monthly means, and these anomalies were used in estimating multidecadal trends. Synoptic variations, the shortest timescale studied, were defined as the departure of daily values from the monthly mean for the relevant month and year.

2.2. Temporal Homogeneity Concerns

[9] It is well known that radiosonde temperature, humidity, geopotential height, and tropopause observations suffer from time-varying biases that confound attempts to extract climate signals, particularly multidecadal trends [*Gaffen*, 1994; *Parker and Cox*, 1995; *Seidel et al.*, 2001; *Redder et al.*, 2004; *Lanzante et al.*, 2003; *Sherwood et al.*, 2005; *Randel and Wu*, 2006]. Although two new radiosonde temperature data sets incorporate homogeneity adjustments to remove these biases [*Free et al.*, 2005; *Thorne et al.*, 2005], they are not suitable for analysis of the tropopause, because they deal only with temperature at specified pressure levels (the so-called mandatory levels) and make no attempt to address the tropopause. In both cases, the

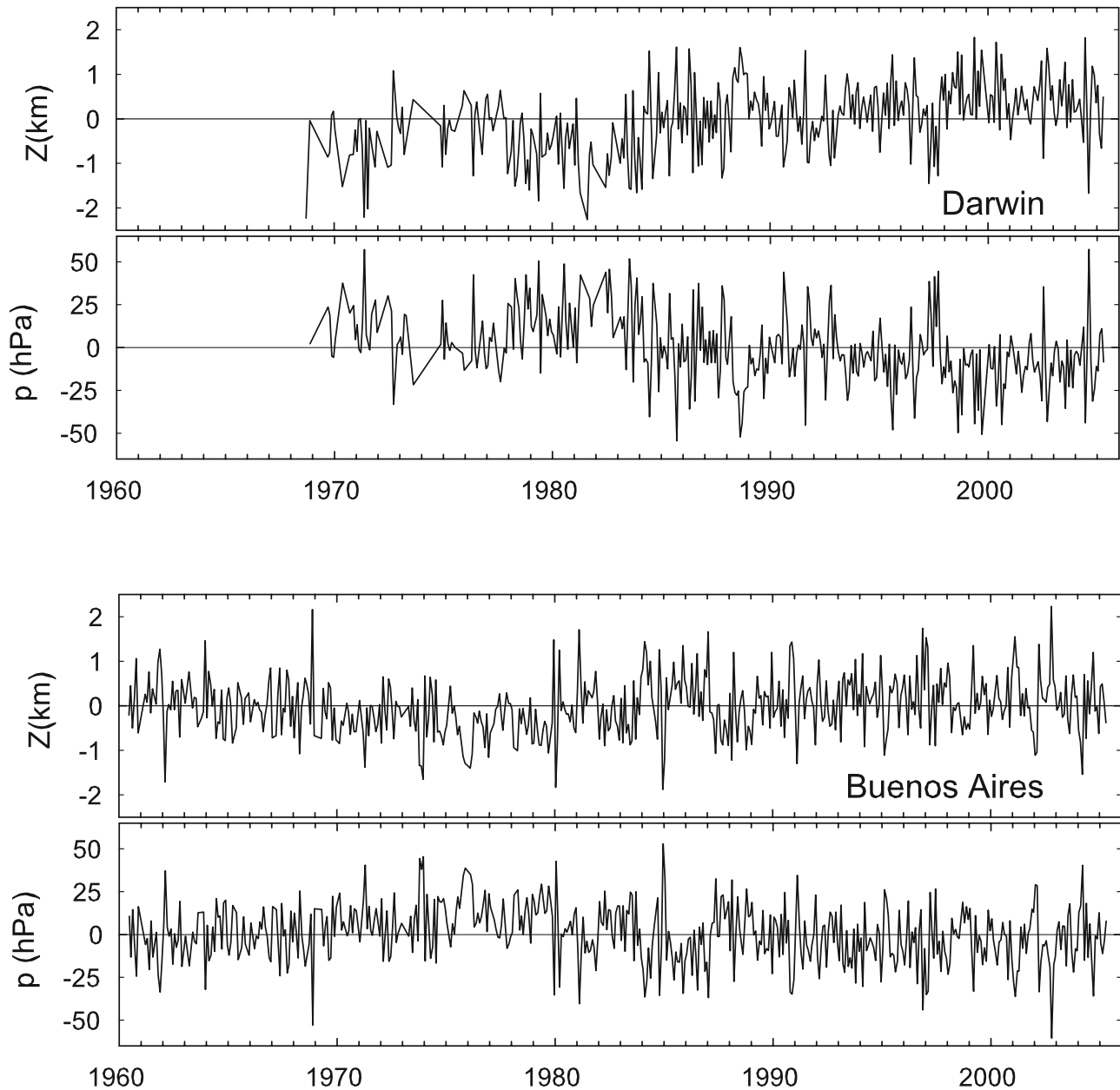


Figure 2. Time series of monthly anomalies (mean annual cycle removed) of tropopause height and pressure at 0000 UTC at Darwin, Australia (top two panels), and at 1200 UTC at Buenos Aires, Argentina (bottom two panels).

adjusted data are monthly anomaly time series, so it is not possible to identify either the daily tropopause location or even its monthly mean level (because the data are anomalies, not actual temperatures, and so lapse rates cannot be computed).

[10] Embarking on this study, our hope was that temporal inhomogeneities affecting the temperature and geopotential height data would not affect observations of the pressure of the tropopause level. Our reasoning was that the location of the “kink” in the temperature sounding associated with the tropopause would not be influenced by high or low biases in the temperature data if pressure were used as the vertical coordinate, since, unlike geopotential height (derived from vertical integration of temperature, humidity and pressure

observations), pressure is independently measured, and it is generally thought that radiosonde pressure observations are more accurate than temperature. Unfortunately, this argument was not valid (see Figure 2), so we were compelled to confront the homogeneity issue directly.

[11] Four sources of information were used to screen stations with inhomogeneous data. First, we relied on the extensive analysis of Lanzante *et al.* [2003], whose “decision files” include the dates of inhomogeneities conservatively or liberally identified by that expert team for each of their 87 stations, for 0000 and 1200 UTC separately, for 1958–1997. Conservatively identified change points at or above the 850 hPa level were grounds for our excluding a station’s data. Second, stations were excluded if there were

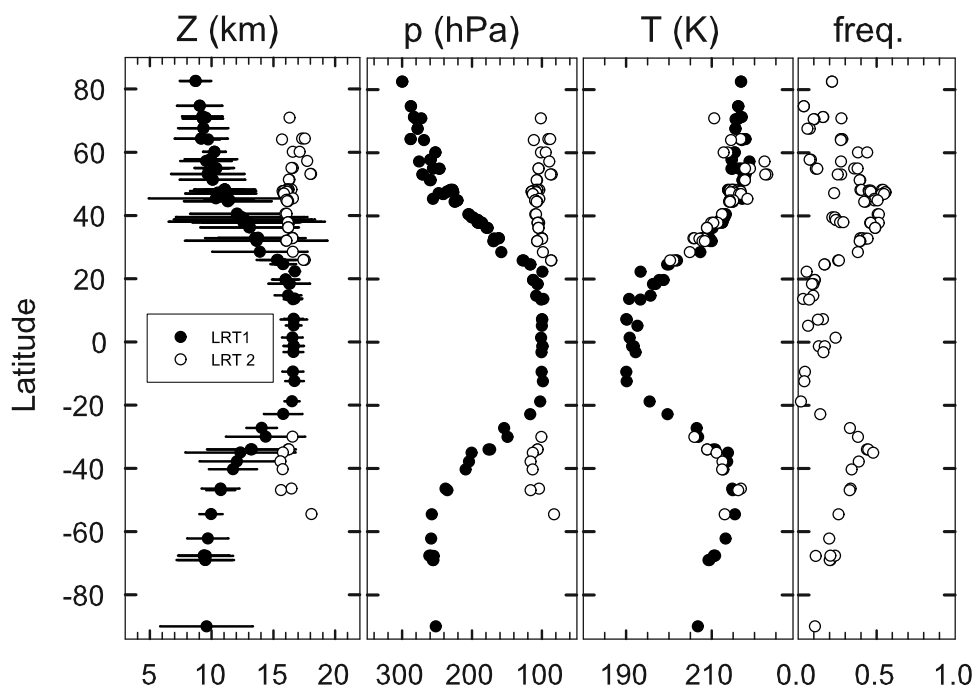


Figure 3. Climatological average height, pressure, and temperature of the first and second lapse rate tropopause (LRT1, solid circles; LRT2, open circles), and the frequency of occurrence of LRT2, for each station and time of observation, as a function of latitude. The amplitude of the mean annual cycle of LRT1 height is indicated by the horizontal lines. Values for LRT2 are shown in the first three panels only for stations where the frequency of LRT2 exceeds 25%.

known instrument changes documented in station history records (*Gaffen* [1993] and subsequent updates by NCDC; *Elliott et al.* [2002]), some occurring after 1997, the end of the *Lanzante et al.* [2003] analysis. Third, we eliminated several stations that *Randel and Wu* [2006] suspected were inhomogeneous on the basis of discontinuities in time series of radiosonde minus satellite observations during 1979–2004. In particular, we excluded any station with a lower stratospheric trend difference between the radiosonde data and satellite data exceeding 0.5 K/decade [*Randel and Wu*, 2006, Table 1]. Fourth, we visually inspected time series of monthly tropopause height and pressure anomalies for each station and found some examples of obvious change points in the data. In many cases, more than one source of information pointed to inhomogeneity problems at a given station. Table 1 (rightmost column) shows whether and why data from each station were suspected of being inhomogeneous, or had excessive missing values.

[12] Figure 2 shows two examples of tropopause height and pressure monthly anomaly time series to illustrate the data homogeneity issue. At Darwin, Australia, there is an abrupt upward jump in tropopause height of about 1 km in about 1984. The strong anticorrelation between LRT pressure and height is reassuring, but the 20–30 hPa LRT pressure jump in 1984 indicates that, if the height change at that time is spurious, pressure data are also affected. A similar feature is evident in the data from Buenos Aires, Argentina, in late 1979. Although no abrupt changes are apparent in the Buenos Aires data after 1980 in Figure 2, *Randel and Wu* [2006] identified this station’s 1979–2004 data as suspect on the basis of comparison with satellite data, and we eliminated them from our main analysis.

[13] We also omitted stations with more than one third of the monthly anomalies missing. On the basis of this criterion and the four indicators of data inhomogeneity, we restricted our analysis to the 25-year period 1980–2004, to best balance the number of stations and the length of record. This left 50 of the original 100 stations (Table 1 and Figure 1), of which 31 had data deemed homogeneous for both 0000 and 1200 UTC. An additional 16 stations with insufficient sampling for trend analysis were included in analyses of climatological statistics (section 3) and zonal-average time series (section 6).

3. Climatological Tropopause Location and Mean Seasonal Variations

[14] The mean structure of the first tropopause has been depicted in numerous previous studies [e.g., *Makover*, 1979; *Hoinka*, 1999]. Figure 3 shows the annual-mean height, pressure and temperature of both the first and second tropopause (LRT1 and LRT2), as a function of latitude. For each station, 0000 and 1200 UTC values are plotted separately if available. Because the LRT2 is not found in all seasons, LRT2 data are presented only for stations at which at least 25% of the soundings had identifiable LRT2 levels. This occurs mainly outside the tropics and polar regions, in the vicinity of the jet streams.

[15] The radiosonde data indicate climatological LRT1 heights decreasing from 16.6 km near the equator to about 9 km in the polar zones, in good agreement with earlier work cited above. Corresponding pressure values are approximately 100 hPa near the equator and increase to about 250 hPa poleward of 60 degrees latitude. The lowest

climatological LRT pressure is 97 hPa at Bangkok, Thailand, and the highest value is 300 hPa at Alert, Canada. The amplitude of the mean seasonal cycle of LRT1 height is shown by the horizontal lines in Figure 3. The amplitude is smallest (0.5–1.7 km) at stations between 20°N and 20°S latitude and has maximum values (2–6 km) in midlatitudes. There is some indication of larger amplitude seasonal variations in the Northern Hemisphere (NH) than in the Southern Hemisphere (SH), which could be related to the greater fraction of land-covered surface there.

[16] In midlatitudes, the location of LRT2, which is not present all year but mainly in winter, is almost identical to the location of the tropical LRT1, 16 km and 100 hPa. Its temperature, however, more closely resembles that of the local LRT1 and never differs by more than 5 K. At most stations, LRT2 is a few Kelvin cooler than LRT1, which is a combined result of the lapse rate between the two levels and the fact that LRT2 statistics are based mainly on fall-winter-spring data, whereas LRT1 data are more representative of the year. At stations near 50°N and 50°S latitude, LRT2 is a few degrees warmer than LRT1, because of temperature inversions between LRT1 and LRT2 in winter.

[17] Figure 4 shows the mean seasonal cycle of the height of LRT1 and LRT2 at five representative stations. Here LRT2 results are shown only if at least 50% of the soundings for a given calendar month had identifiable LRT2 levels, so that at equatorial Nairobi, Kenya, it is never shown, and at Bet Dagan, Israel, and Capetown, South Africa, in midlatitudes, it is not apparent in summer months. Figure 3 and results from the full network of stations confirm that when the LRT2 is present at extratropical stations it is located close to 16 km, the height of LRT1 in the tropics (e.g., Nairobi), where the seasonal variation is generally less than 1 km and peaks in NH winter/spring, consistent with findings presented by *Seidel et al.* [2001] from a larger set of tropical stations. At midlatitude stations, LRT1 reaches its maximum height in local summer, following the annual cycle of tropospheric temperature; the patterns at Bet Dagan and Capetown are typical.

[18] At polar stations, the situation is more complex, as discussed in detail by *Wong and Wang* [2000], using a climate model and NCEP/NCAR reanalysis data, and *Highwood et al.* [2000] and *Zängl and Hoinka* [2001], who analyzed ECMWF reanalysis data. The interplay of radiative and dynamical processes in both the troposphere and stratosphere results in three different patterns of seasonal variability [*Zängl and Hoinka*, 2001]. The examples from Point Barrow, Alaska, and the Japanese Antarctic station at Syowa (Figure 4) are typical of two of these patterns, with a single annual wave showing maximum tropopause height in NH summer. According to *Zängl and Hoinka* [2001], this pattern is typical in the south polar region and in the subpolar parts of eastern Siberia and North America. They find a double-wave pattern, with smaller amplitude variations, in other NH subpolar regions and in the high Arctic. In our network, the majority of NH high-latitude stations, including Point Barrow (Figure 4) have a single-wave seasonal variation, but we find a suggestion of double-wave patterns at Alert, Jan Mayen, Sodankyla, Angmagssalik, Lerwick, and Baker Lake (see Table 1 for station locations), in

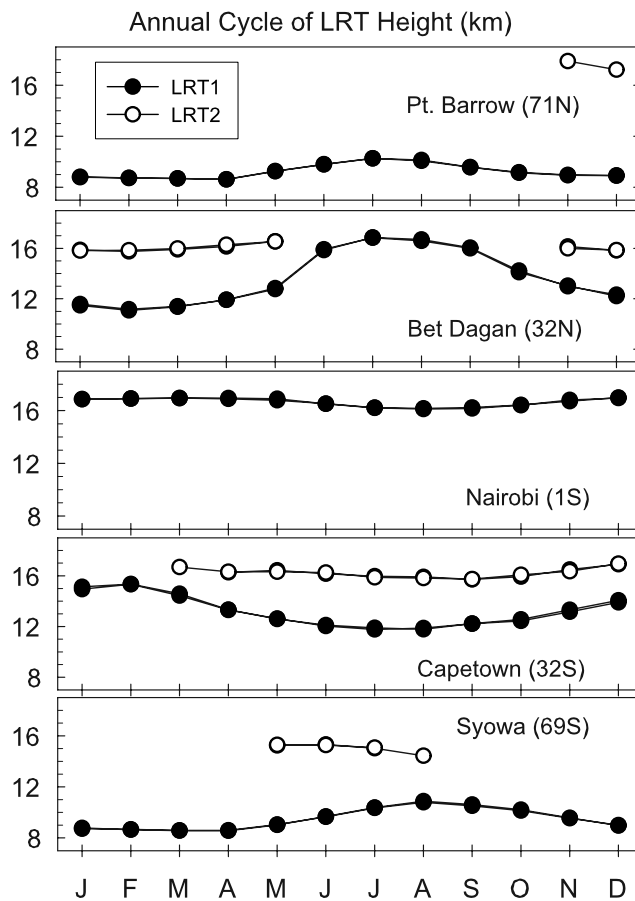


Figure 4. Climatological mean annual cycle of the height of the first and second lapse rate tropopause (LRT1 and LRT2) at five stations. The height of LRT2 is shown only if it was identified in at least 50% of the soundings for the month.

general agreement with the spatial patterns identified by *Zängl and Hoinka* [2001].

4. Typical Magnitudes of Tropopause Height and Pressure Variations

[19] Figure 5 compares the variability of LRT height (left) and pressure (right) at different timescales. For synoptic (day-to-day), climatological annual cycle (month-to-month), and monthly anomaly variations, we show the distribution among stations of the standard deviations of the relevant time series. The long-term change estimates are distributions of the magnitudes of the changes in LRT pressure or height over 1980–2004, based on linear trends. Results in Figure 5 are based on all stations but primarily represent the extratropics. Specific tropical-extratropical differences are noted in turn.

[20] The largest LRT variations occur on the synoptic scale. The standard deviations of day-to-day LRT height changes have median values of about 1.4 km (with a range of 0.5–1.9 km). The corresponding median standard deviation of LRT pressure is 45 hPa (range 9–57 hPa). The tropical stations have synoptic-scale standard deviations in the lowest quartile of the distribution.

[21] Tropopause height standard deviations associated with the climatological annual cycle have a median value

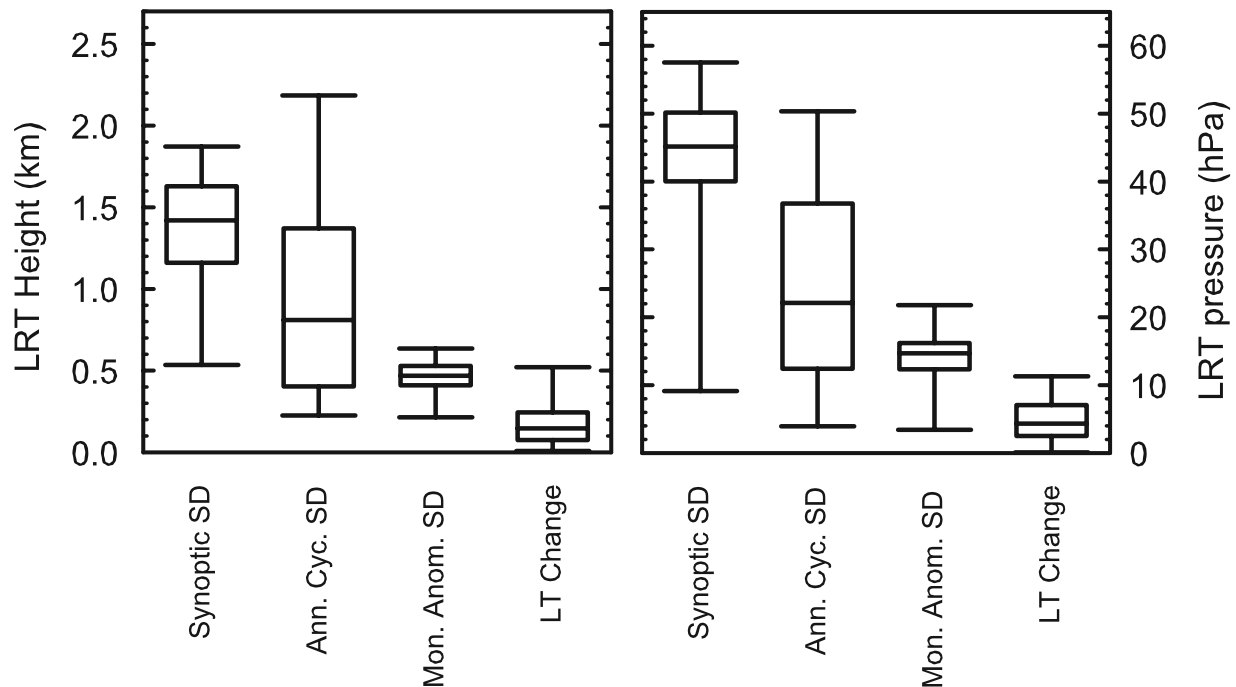


Figure 5. Comparison of the variability of lapse rate tropopause (left) height and (right) pressure at different timescales. The first three box plots in each panel show the distribution of the standard deviations of tropopause height or pressure associated with (from left to right) daily synoptic variations for the complete length of record, monthly variations associated with the climatological mean annual cycle, and variations of monthly anomalies for the complete length of record. The fourth (rightmost) box plot in each panel shows the distribution of the absolute magnitudes of the net (1980–2004) change in tropopause height or pressure, based on linear trends. Box and whisker plots show minimum, maximum, and 25th, 50th (median), and 75th percentiles of values obtained at individual stations and observation times.

of 0.8 km (and a range of 0.2–2.2 km) and so are about half the size of synoptic variations. The annual cycle standard deviations of LRT pressure have a median value of 22 hPa. The midlatitude stations have the highest seasonal variability, while variability of LRT height and pressure at tropical stations is below the median values (Figure 3).

[22] The standard deviations of monthly anomalies range from 0.2 to 0.6 km for LRT height and from 3 to 22 hPa for LRT pressure, again with larger variations outside the tropical belt. These are less than half the magnitude of the variability on synoptic timescales, which are smoothed in the creation of monthly anomalies and do not persist long enough to dominate the monthly values.

[23] The 25-year trends computed from the monthly anomaly data have maximum magnitudes of 0.5 km, or 11 hPa, but more than half the stations show long-term changes less than 0.2 km or 4 hPa. These are an order of magnitude smaller than the vertical resolution of contemporary global climate models and of atmospheric reanalyses. As discussed by *Santer et al.* [2003a], 50-hPa resolution near the tropopause is typical, which corresponds to about 2 km in height coordinates.

5. Covariations on Day-to-Day and Monthly Timescales

[24] On multidecadal timescales, the global tropopause height rises with a warming troposphere and cooling stratosphere, in both climate models and reanalysis data sets

(*Sausen and Santer* [2003] and *Santer et al.* [2003a, 2003b, 2004]; see also the discussion by *Shepherd* [2002]). These results are consistent with those of *Hoinka* [1999], who analyzed ECMWF reanalysis, radiosonde, and satellite Microwave Sounding Unit data and found a positive correlation between global tropopause height and tropospheric temperature. Similarly, *Kiladis et al.* [2001], analyzing radiosonde and NCEP/NCAR reanalysis data, report (1) an ENSO signal in the tropical tropopause, with higher tropopause heights associated with warmer sea surface temperatures [see also *Reid and Gage*, 1985; *Randel et al.*, 2000], and (2) extratropical tropopause temperature changes that are positively correlated with temperature anomalies in the stratosphere and negatively correlated with those in the troposphere. They attribute the tropical relationship to convection and the extratropical to quasi-geostrophic Rossby waves. However, they suggest that climatological tropopause features and their seasonal variations may show different relationships, and may be due to different processes, including radiative effects and wave driving in the middle atmosphere.

[25] In this section and the next, we investigate the covariability of tropopause height and the vertical temperature profile at different timescales and with the vertical resolution available from the radiosonde data. Figure 6 shows the vertical profiles of correlations between tropopause height changes and temperature changes, at monthly and synoptic (day-to-day) timescales, for three sample stations, as well as the pressure level of the local climatological mean

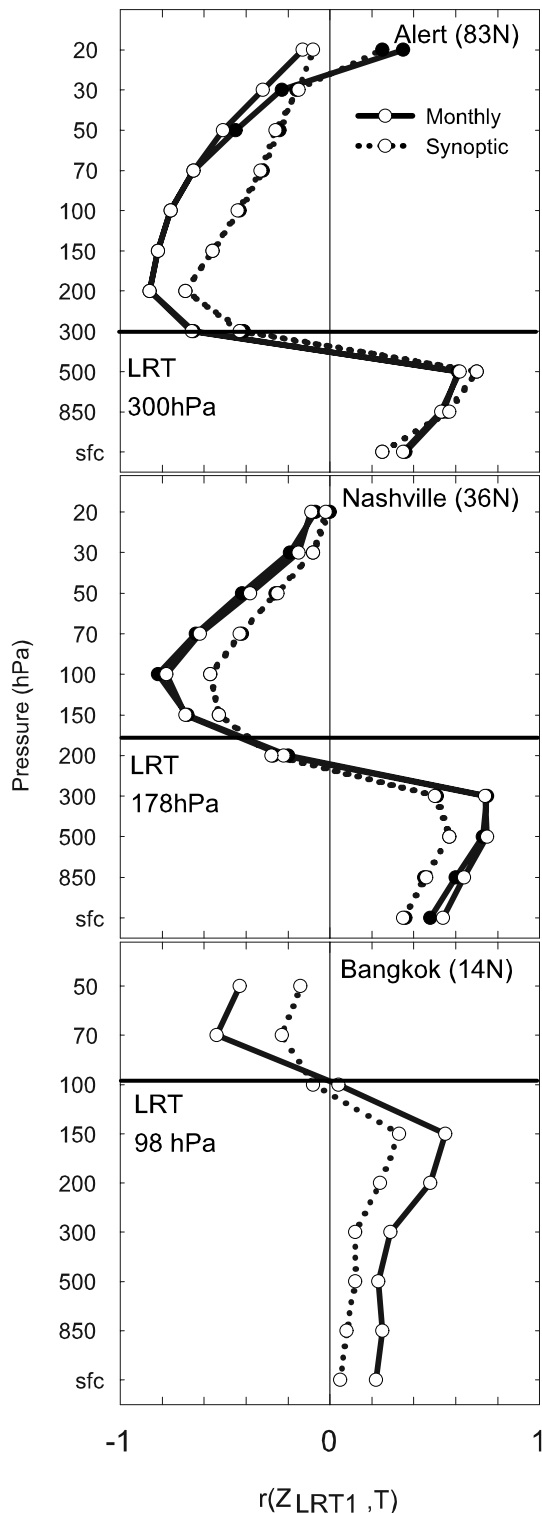


Figure 6. Vertical profiles of the correlation between temperature anomalies at a given level and tropopause height anomalies at three stations, (top) Alert, (middle) Nashville, and (bottom) Bangkok. Correlations based on monthly and synoptic anomalies are indicated by solid and dotted lines, respectively. Correlations based on 0000 and 1200 UTC anomalies are indicated by solid and open circles, respectively, for Alert and Nashville. The position of the climatological lapse rate tropopause (LRT) is shown by horizontal lines.

tropopause. Figure 7 (top) shows summary statistics of the monthly correlations from all the stations for which we did not have data inhomogeneity concerns (indicated by a 3, 4, or 5 in Table 1). Linear regression coefficients between LRT height and temperature are shown in the bottom panels of Figure 7, expressing LRT height changes in terms of temperature change at each pressure level.

[26] Each of these profiles has a characteristic “S” shape, with negative correlations (regressions) above the tropopause and mainly positive values below. The strongest negative and positive correlations occur in the lower stratosphere and upper troposphere, respectively. Correlations based on synoptic and monthly anomaly data have similar vertical structure, but the latter are often stronger than the former (Figure 6). There is generally excellent agreement between correlations based on 0000 and 1200 UTC data at the same station (Figure 6).

[27] For synoptic scales in extratropics, the observed relationships between tropopause height and vertical temperature structure are consistent with balanced dynamical structure in midlatitude cyclones and anticyclones [see *Hoskins et al.*, 1985, Figure 15]. In particular, balanced cyclonic structure is characterized by a low tropopause, in association with a relatively cold troposphere and warm lower stratosphere; conversely, balanced anticyclones have a relatively high tropopause, warm troposphere and cold lower stratosphere. The fact that the monthly timescale anomalies in Figure 7 exhibit similar correlations (and regression values) to synoptic scales may be explained if the monthly anomalies are primarily due to the accumulated effects of synoptic variability.

[28] Tropopause height is less strongly correlated with the temperature profile in the tropics than in the extratropics (Figure 7, top), particularly at levels far from the tropopause. In the tropics, 300 hPa temperatures show the strongest positive correlations (median value 0.47), and 100 hPa temperatures show the strongest negative correlations (median -0.60), although the exact levels of maximum correlation vary from station to station, depending on the local mean tropopause level. At 50 hPa and above, and at the surface and 850 hPa level, tropical correlations are almost always less than 0.4 in absolute magnitude. In the extratropics, strongest positive correlations are at 500 hPa (median 0.78) and strongest negative correlations are at the 150 and 100 hPa levels (medians -0.71).

[29] The regression values indicate that the tropical tropopause rises about 1 km per 1 degree warming of the upper troposphere and about 2 km per 1 degree cooling of the lower stratosphere. For the extratropics, a 1 degree warming at 500 hPa, or a 1 degree cooling at 200 hPa, is associated with a 3 km tropopause rise. Thus the extratropical tropopause appears to be more sensitive to temperature changes than the tropical tropopause. However, when interpreting these regression results, it is important to recognize that the troposphere does not warm independently of the stratosphere cooling on synoptic or monthly timescales, because of the balanced dynamical structures discussed above.

6. Trends in Tropopause Height and Temperature

[30] Tropopause height trends during 1980–2004, estimated by linear regression, and their ± 2 -sigma confidence

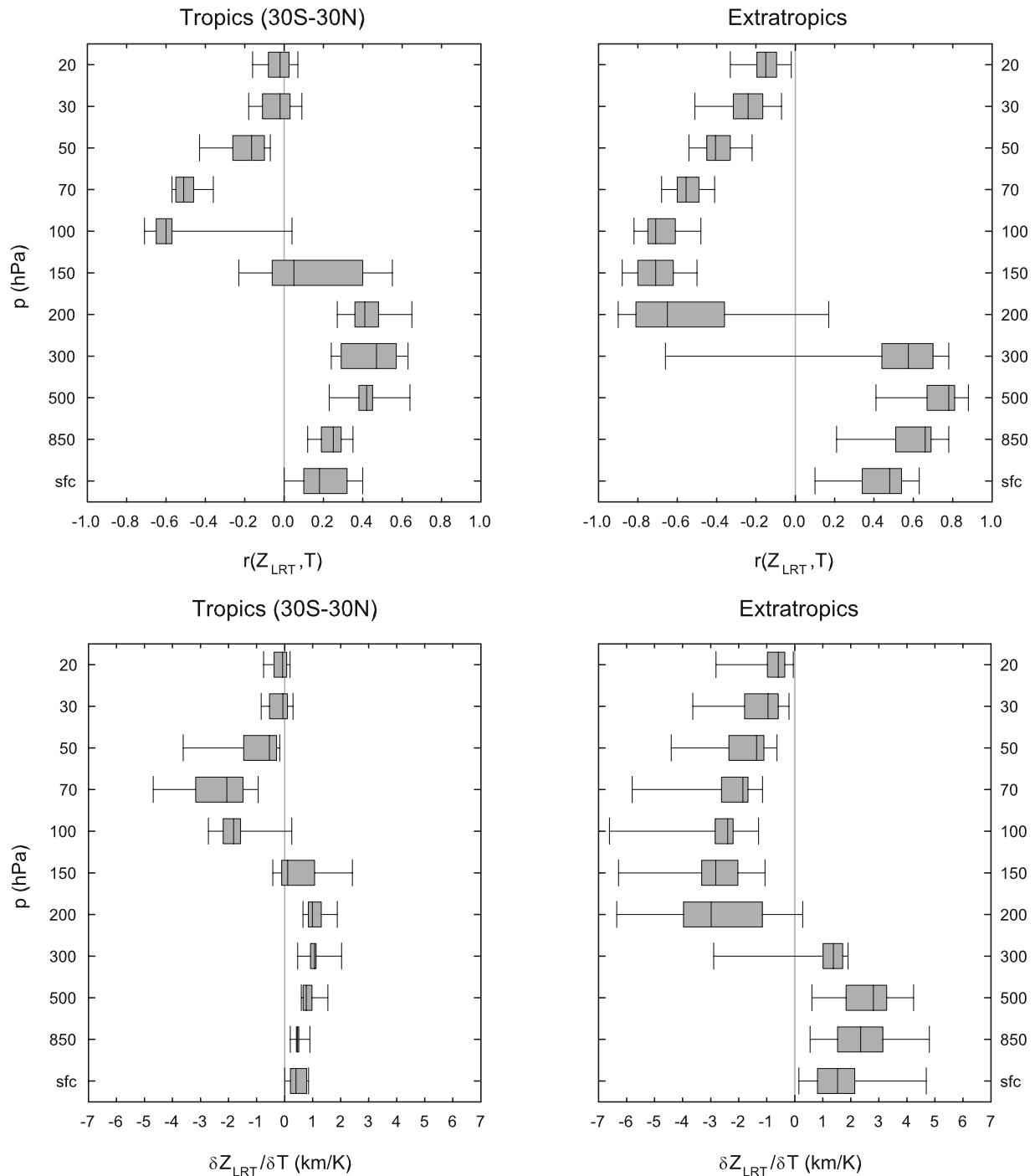


Figure 7. Vertical profiles of the distribution of (top) correlation coefficients and (bottom) regression coefficients (km/K) between monthly anomalies of temperature at a given level and tropopause height. Panels at left are for tropics (30°S to 30°N), and panels at right are for extratropics. Each box and whisker plot is based on all available stations and times of observation and show minimum, maximum, and 25th, 50th, and 75th percentile values.

intervals (taking into account the effect of temporal auto-correlation on the number of independent values in each series [Santer *et al.*, 2000]), are shown in Figure 8. Here, and only here (Figure 8, left), we show results based on the full original station network (Table 1) as well as results based on the 50 stations (indicated by a 3, 4, or 5 in Table 1) whose homogeneity we had no reason to question (right

panel, with one half the horizontal axis range of the left). There is more scatter in the results from the full network, and some notable outliers, with trends less than -500 m/decade. The more restricted network shows remarkably consistent trends, with positive values at almost all stations and observation times, with a range of -43 to $+209$ m/decade, and an average value of 62 m/decade. However, the

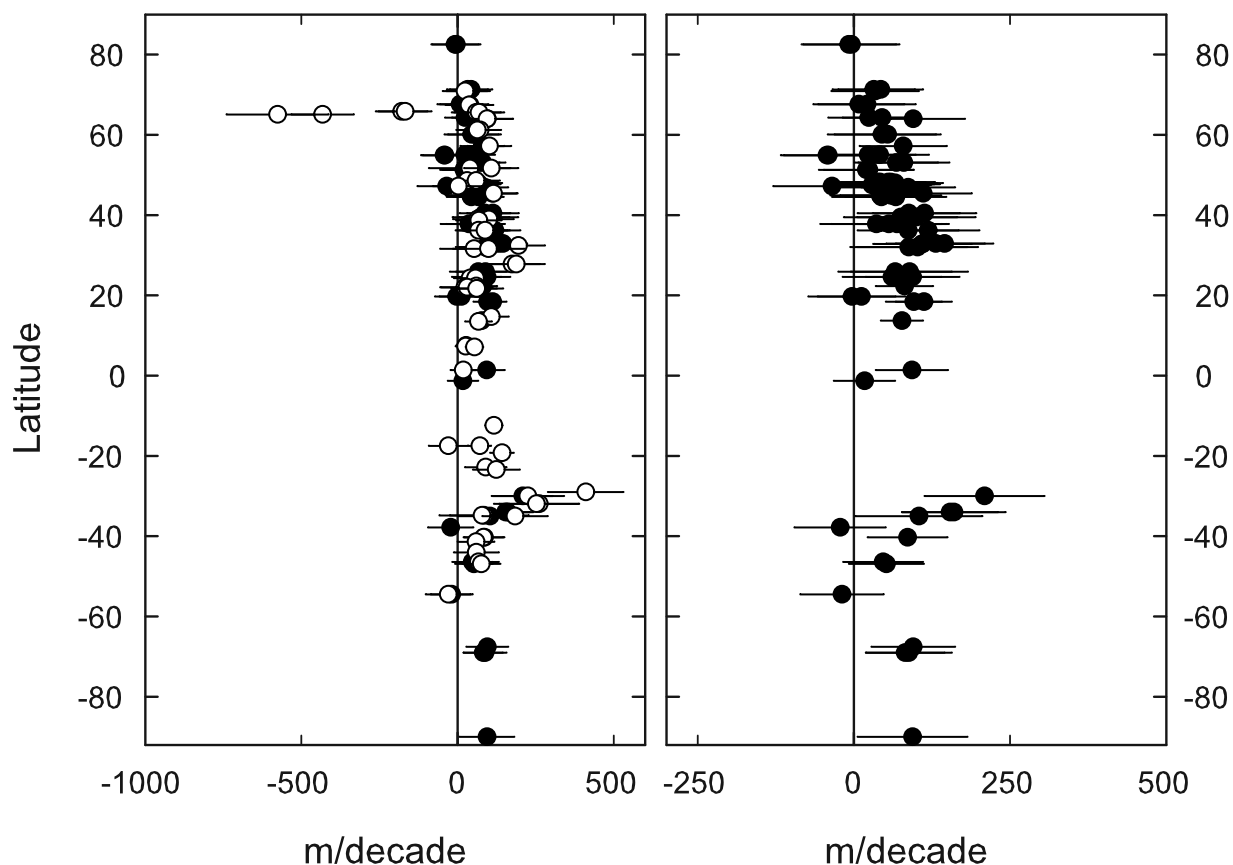


Figure 8. Tropopause height trends (m/decade) for 1980–2004 as a function of latitude. Error bars show ± 2 -sigma confidence intervals. Each point represents a different station and time of observation. (left) Trends at stations indicated by 1, 3, 4, or 5 in Table 1, with open circles indicating stations and observation time with inhomogeneous time series. (right) Results only for stations with no discernible inhomogeneities (indicated by 3, 4, or 5 in Table 1). Note the different horizontal axis scales.

trend confidence intervals for many of the individual stations overlap zero.

[31] Averaging time series from different stations and observation times to form seven zonal mean time series in 25.7-degree latitude bands reduces the noise and increases the statistical significance of the trends. Figure 9 shows the seven zonal time series, as well the global average, based on area weighting of the zonal series. In creating these zonal time series, we included data from all stations for which we did not suspect the data were inhomogeneous, even if the time series had gaps that precluded computation of trends at that station. Thus all stations except those indicated by a “1” in Table 1 are included in the zonal means.

[32] Figure 10 shows trends in zonal-mean tropopause height, pressure, and temperature, as well as the number of time series used per zone. Clearly, the NH extratropics is the best sampled region, which leads to generally smoother time series (Figure 9) and smaller trend confidence intervals (Figure 10). In all zones, we find an increase in tropopause height ranging from 10 to 119 m/decade and a decrease in tropopause pressure ranging from 0.8 to 2.7 hPa/decade. The largest tropopause height and temperature trends are in the SH subtropical zone (where a large trend at Durban, South Africa, dominates this poorly sampled region), and the smallest are in the NH polar region. In all but the most northerly zone, tropopause temperature trends are negative,

with the strongest cooling (0.78 K/decade) in the SH subtropical zone.

[33] To test the sensitivity of the zonal trends to station sampling, we also computed zonal means using only the stations with sufficient data to allow computation of individual station trends (indicated by a 3, 4, or 5 in Table 1). Figure 10a shows that tropopause height trends from these two networks are in good agreement over most of the globe. The differences are largest in the tropics, where the more restrictive network yields a larger trend by about a factor of 2, but the two estimates (shown by solid circles and open squares) are always within each other’s uncertainty estimates.

[34] We have also computed tropopause trends on a seasonal basis (not shown). The increase in LRT height is found in all four seasons and all seven zonal bands, with three exceptions. Trends are near zero in JJA in the tropical and SH midlatitude bands, and there is a statistically significant LRT height decrease in the North Polar zone in DJF.

[35] Trends based on the global time series indicate highly statistically significant tropopause changes during 1980–2004. The height of the LRT increased at a rate of 64 ± 21 m/decade (yielding a net rise of 160 m over the 25-year period), with an associated pressure decrease of 1.7 ± 0.6 hPa/decade (net change of -4.2 hPa), and a temperature

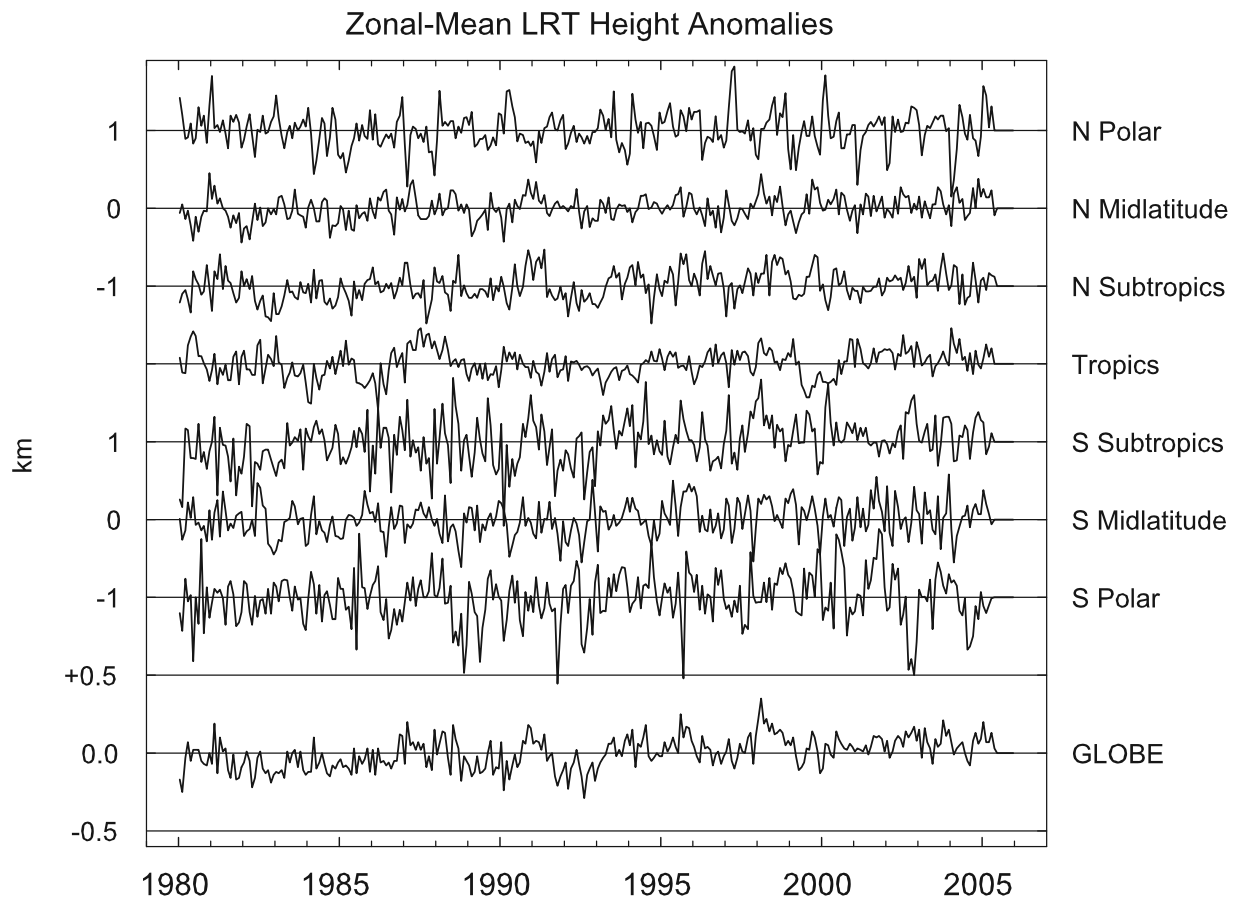


Figure 9. Monthly anomalies of tropopause height for the globe (bottom trace) and in seven 25.7-degree latitude bands for 1980–2004. Each tick mark represents 1 km on the vertical axis, except for the global time series, where each represents 0.5 km.

decrease of 0.41 ± 0.09 K/decade (net change of -1.0 K). These LRT changes were accompanied by a slight (not statistically significant) warming of the tropospheric 850–300 hPa layer of 0.036 ± 0.066 K/decade and a strong cooling of the stratospheric 100–50 hPa layer of 0.77 ± 0.21 K/decade.

[36] Previous studies, based on a variety of data sources and for different regions, report different tropopause trends. Global tropopause trends have been estimated exclusively from reanalysis data. *Sausen and Santer* [2003] and *Santer et al.* [2003a] report trends in tropopause pressure of -1.82 hPa/decade for 1979–1997 and -2.16 hPa/decade for 1979–2000, respectively, in the NCEP/NCAR reanalysis. *Santer et al.* [2003a] also report a trend of -1.13 hPa/decade in the 15-year ECMWF reanalysis for 1979–1993, an order of magnitude larger than the estimates of *Hoinka* [1998, 1999], who reports trends of -0.1 and $+0.1$ hPa/decade. Using the improved 40-year ECMWF reanalysis, *Santer et al.* [2004] find global trends of -2.36 ± 0.47 and -2.66 ± 0.48 hPa/decade for 1979–2001, using data with two different vertical resolutions. As shown in Appendix A, we obtain a similar global LRT pressure trend difference (0.4 hPa/decade) by reducing the vertical resolution of the radiosonde data, although some local differences are much larger.

[37] If we limit our analysis to the same data periods (but starting in 1980 rather than 1979) as used in those studies,

we obtain global tropopause pressure trends of -0.77 ± 1.42 , -1.60 ± 1.00 , -1.89 ± 0.81 , and -1.83 ± 0.75 hPa/decade for 1980–1993, 1980–1997, 1980–2000, and 1980–2001, respectively. These radiosonde trend confidence intervals are large enough to encompass most of the published tropopause trends in reanalyses. However, the radiosonde-based trends are smaller than the reanalysis trends reported by *Sausen and Santer* [2003] and *Santer et al.* [2003a, 2004] (except for the 15-year ECMWF trends), but much larger than those reported by *Hoinka* [1998, 1999].

[38] In the tropics, *Randel et al.* [2000] found a decrease in tropopause temperature (~ 0.5 K/decade) and pressure (~ 0.4 hPa/decade) in 1979–1997 radiosonde data, but no trend during the same period in NCEP/NCAR reanalysis data. The radiosonde results are consistent with *Seidel et al.* [2001], who report a 1978–1997 increase in tropopause height of ~ 20 m/decade, decrease in pressure of ~ 0.5 hPa/decade, and cooling of ~ 0.5 K/decade, on the basis of radiosonde data in the 15°S to 15°N equatorial zone. The 1980–1997 trend in our tropical zone is -0.72 ± 1.5 hPa/decade. The difference may be due to the poorer spatial sampling in this analysis compared with the earlier studies which focused on the tropics; here we have only ten station time series contributing to the tropical zonal mean.

[39] Several studies have reported regional tropopause changes. *Thompson et al.* [2000] attribute an increase in

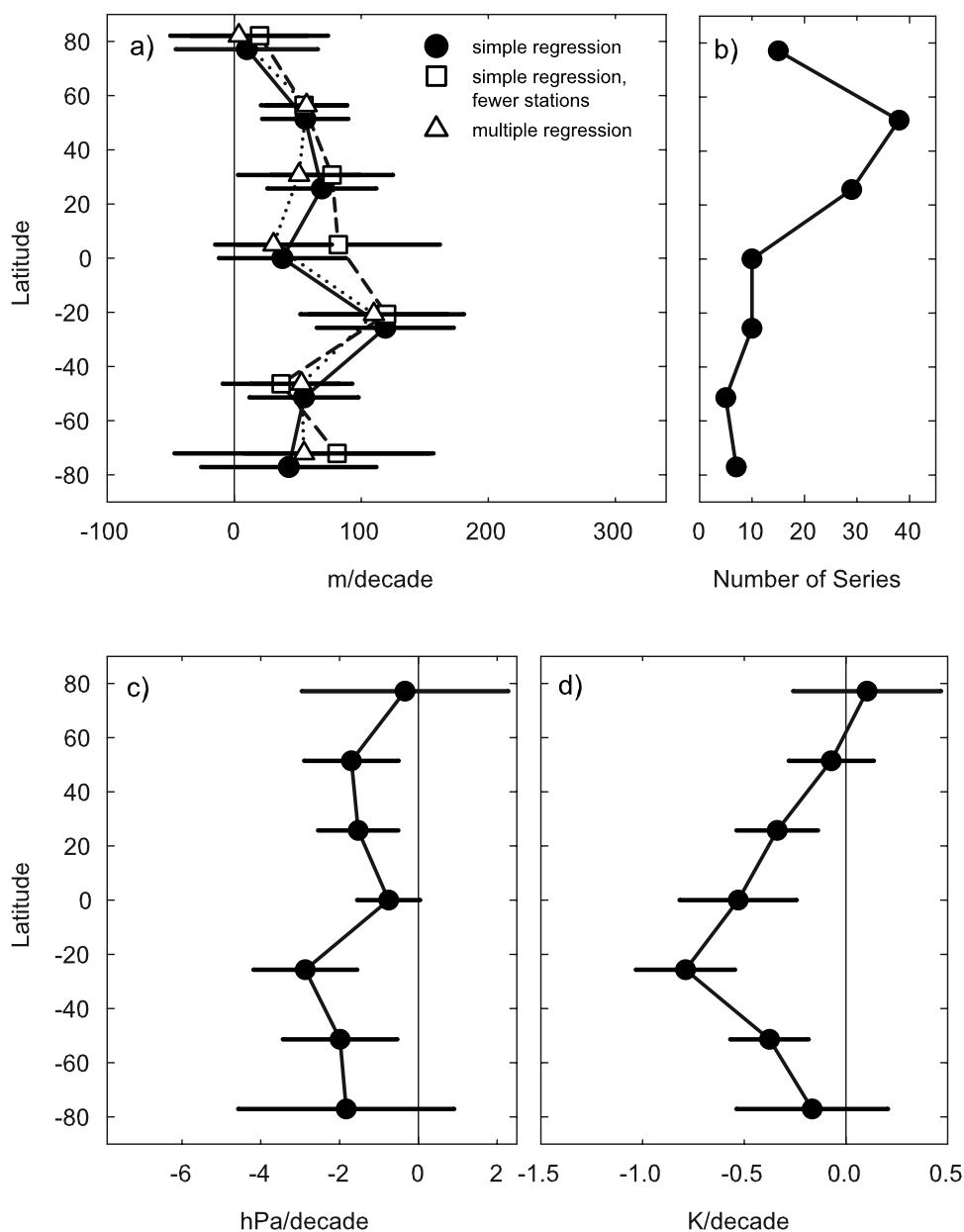


Figure 10. Trends in zonal-mean tropopause height (Figure 10a), tropopause pressure (Figure 10c), and tropopause temperature (Figure 10d) as a function of latitude, and the number of station time series used to create the zonal time series (Figure 10b). Error bars indicate the ± 2 -sigma confidence intervals for the trend estimates. For tropopause height (Figure 10a), trends are estimated via simple linear regression (solid circles) and multiple regression (open triangles) using time series based on all station data in the relevant 25.7-degree latitude zone and via simple linear regression using time series based only on stations with at least 67% of nonmissing monthly anomaly data (open squares).

wintertime tropopause height over Europe and Canada, as seen in NCEP/NCAR reanalysis data for 1968–1997, in part to changes in the Arctic Oscillation. *Añel et al.* [2006] also find a strong signal of the Northern Annular Mode in the variability of radiosonde-derived tropopause height over Eurasia, and note that computed trends in tropopause height are very sensitive to decisions regarding data quality and homogeneity. *Forster and Tourpali* [2001] analyzed ozone-sonde data at eleven NH sites and found tropopause height increases of 330 to 520 m during 1970–1996/1997, with

associated trends in ozone profile, consistent with earlier work by *Steinbrecht et al.* [1998] focusing on data from Hohenpeissenberg. *Nagurny* [1998] reports an increase of ~ 0.3 km in the height of the Arctic tropopause, on the basis of radiosonde data from drifting stations, and *Highwood et al.* [2000] find Arctic tropopause pressure decreases of 5 to 14 hPa (with largest trends in winter, associated with the Arctic Oscillation) over 1965–1990. *Varotsos et al.* [2004] report an upward trend in tropopause height and a decrease in tropopause temperature over Greece during 1984–2002,

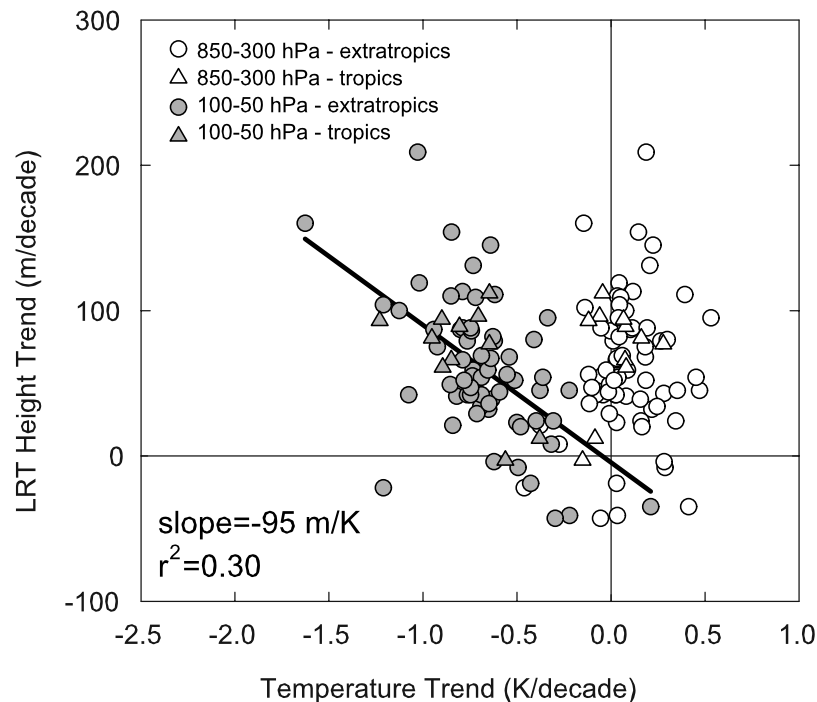


Figure 11. Scatterplot showing the relationships between tropopause height trends and temperature trends in the troposphere (850–300 hPa, open symbols) and stratosphere (100–50 hPa, solid symbols). Each point represents a different station and observing time, with triangles for tropical (30°S to 30°N) stations and circles for extratropical stations. The sloped line shows the regression relation for the stratospheric temperature trends.

and discuss associated trends in column ozone. *Chakrabarty et al.* [2000] report an increase in tropopause height over India of 0.57 to 1.13%/decade (about 140 m/decade) with radiosonde data periods ranging from 26 to 32 years, beginning in 1965.

[40] The relationships between LRT height trends and temperature trends are shown in the scatterplot in Figure 11. There is no clear relationship between the local strength of tropospheric (850–300 hPa) temperature trends and that of LRT height trends. However, stratospheric (100–50 hPa) temperature trends and LRT height trends are anticorrelated and the data indicate LRT height increases of about 100 m per degree K of stratospheric cooling, with $r^2 = 0.30$. The relationship is almost identical within the tropics (triangles in Figure 11) and the extratropics (circles). The ratio of the magnitude of changes in temperature and LRT height is smaller, by a factor of 20 to 30, than the corresponding relationships between LRT height variations and stratospheric temperature variations on monthly timescales, discussed in the previous section (Figure 7).

[41] Recall, too, that on these shorter timescales, LRT height is significantly correlated with tropospheric temperature, which is not the case for trends, although this finding may be largely due to the weakness of the tropospheric trends in these data. The tropospheric trends are “weak” in two senses of the word. First, they are small and in many cases not statistically significantly different from zero. Second, despite our attempts to screen out stations with temporally inhomogeneous data (as discussed in section 2.2) the tropospheric time series may contain small inhomogeneities which recent studies suggest might lead to an underestimate of

tropospheric warming [*Lanzante et al.*, 2003; *Free et al.*, 2005; *Sherwood et al.*, 2005; *Randel and Wu*, 2006].

[42] The increase in global LRT height is evident in the time series in Figure 9 (bottom trace), which also shows other components of interannual variability. To ascertain the nature of these variations, we performed a multiple regression analysis of the global and zonal tropopause height monthly anomaly time series including proxies to model the quasi-biennial oscillation (QBO) and El Niño–Southern Oscillation (ENSO). We use the 70 hPa zonal winds at Singapore as a QBO proxy [*Naujokat*, 1986], which we find to be the best level for correlations with the global tropopause (somewhat stronger than the 50 hPa level). ENSO variations are derived using the Multivariate ENSO Index (http://www.cdc.noaa.gov/people/klaus.wolter/MEI/mei.html#ref_wt1; *Wolter and Timlin* [1998]). We also included proxies for 11-year solar cycle variability and stratospheric aerosol loading due to volcanic eruptions, but these did not yield statistically significant results. *Santer et al.* [2004] find tropopause height decreases following the El Chichón and Pinatubo eruptions in both ECMWF and NCEP/NCAR reanalyses. These differing results may be related to differences in statistical method used to identify the volcanic signal or to discrepancies between reanalysis and radiosonde depictions of the signal.

[43] Tropopause height regression coefficients and their ± 2 sigma confidence intervals for the QBO proxy are shown in Figure 12. The QBO exhibits a coherent global signature in tropopause height, with out-of-phase variations between the equator and midlatitudes of both hemispheres, a pattern first documented by *Angell and Korshover* [1964].

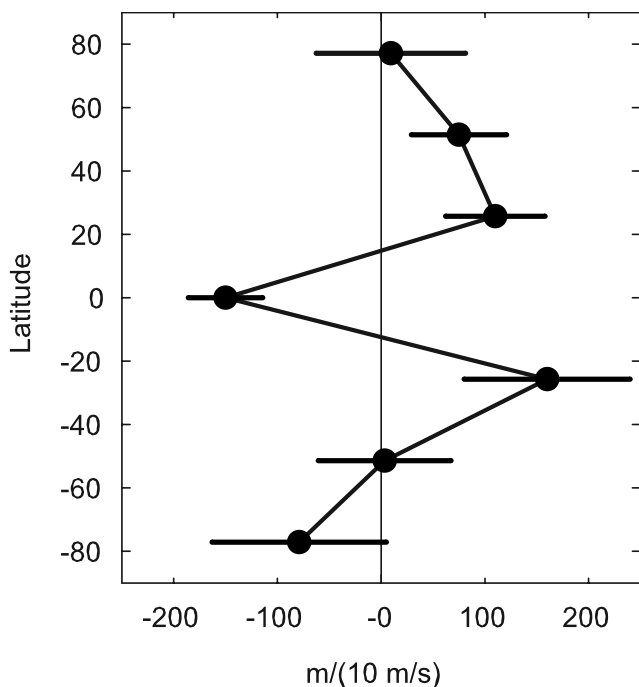


Figure 12. Coefficient of regression between zonal-mean tropopause height anomalies and the quasi-biennial oscillation, as measured by 70 hPa winds over Singapore, as a function of latitude. Error bars show ± 2 -sigma confidence intervals.

Tropopause height variations at the equator are out of phase with zonal winds at 70 hPa. These wind variations are in thermal wind balance with temperature fluctuations in the lower stratosphere, so that the equatorial tropopause height is negatively correlated with the lower stratospheric QBO temperature signal [Reid and Gage, 1985; Randel *et al.*, 2000]. Previous studies [e.g., Randel *et al.*, 1999] have revealed an out-of-phase latitudinal structure in each hemisphere as a characteristic pattern of QBO-related temperature variations in the lower stratosphere. That the global QBO-related tropopause height variations show a similar pattern (Figure 12) suggests that tropopause height is closely coupled to lower stratosphere temperatures. To quantify this relationship, we performed similar QBO regressions with temperature time series, and then calculated the ratio of tropopause height (from Figure 12) to temperature QBO signals. The QBO temperature regressions show significant results for pressure levels in the lower stratosphere (with structure similar to that in Figure 12), and the resulting ratio of tropopause height to temperature changes is near -200 m/K. This ratio is similar in magnitude to the trend ratio estimated in Figure 11, but a factor of 10 smaller than the synoptic and monthly ratios in Figure 7.

[44] The ENSO signal obtained in this analysis (not shown) is only statistically significant in the tropical zone and would suggest a coherent variation of tropopause height within that band. However, the spatial pattern of the ENSO signal in the tropical tropopause has a predominant east-west seesaw pattern [Randel *et al.*, 2000; Kiladis *et al.*, 2001; Gettelman *et al.*, 2001] that is poorly sampled with our limited station network.

[45] The multiple regression analysis also included a trend term, and the results, shown in Figure 10a, are in excellent agreement with the trends computed using simple linear regression. This suggests that the upward tropopause trends found in each of the zonal band are not attributable to variations associated with ENSO, the QBO, solar output, or volcanic aerosols.

7. Summary

[46] This study has focused on quantifying tropopause variability observed in global radiosonde data and understanding correlations between tropopause height and temperatures throughout the vertical profile. We have analyzed variability over a range of timescales (synoptic through interannual changes), and compare the results across scales. Because we want to highlight long-term changes in tropopause height, temporal inhomogeneities in radiosonde data have been carefully considered. We relied on several sources of information to screen station data for homogeneity, which reduced the initial network of 100 stations with data extending back to the late 1950s to a set of 51 stations for the 25-year period 1980–2004.

[47] The climatological height of the first lapse rate tropopause (LRT) varies smoothly with latitude, from 9 km near the poles to 16 km in the tropics, corresponding to pressures of 300 to 100 hPa, consistent with previous results. In midlatitudes a second LRT is found at ~ 16 km (~ 100 hPa), although it is not often present in summer. In extratropical regions the annual cycle of LRT height peaks in summer, whereas in the tropics the annual cycle of LRT height is very small.

[48] LRT height and pressure vary on synoptic (day-to-day), monthly, seasonal, and multidecadal timescales. Synoptic variability is the largest, with standard deviations of approximately 1–2 km or 20–50 hPa. Variability associated with both the annual cycle and monthly anomalies is less than half the synoptic variability, and in both cases is smaller in the tropics than extratropics. LRT changes over the 25 years analyzed have maximum magnitudes of 0.5 km, or 12 hPa, and median values of 0.2 km or 4 hPa. We note that these observed changes are much smaller than the vertical resolution of contemporary global climate models and of atmospheric reanalyses [Santer *et al.*, 2004].

[49] On synoptic and monthly anomaly timescales, tropopause height variations are anticorrelated with stratospheric temperature variations and positively correlated with tropospheric temperature variations. Correlations are stronger in the extratropics than in the tropics, for the upper troposphere (500–300 hPa) than for the lower troposphere, and for the lower stratosphere than for the middle stratosphere. The level at which correlations switch from negative to positive is very close to the local mean LRT pressure. These observed relationships for extratropical synoptic scales are characteristic of the balanced dynamical structure of midlatitude cyclones and anticyclones, and the monthly anomalies likely reflect the accumulated effects of synoptic variability. Regression analysis indicates that the extratropical tropopause is more sensitive to temperature changes than the tropical tropopause. In both regions monthly anomalies of tropopause height are more sensitive to stratospheric temperature change than tropospheric, rising 2–3 km per degree cooling of the lower stratosphere.

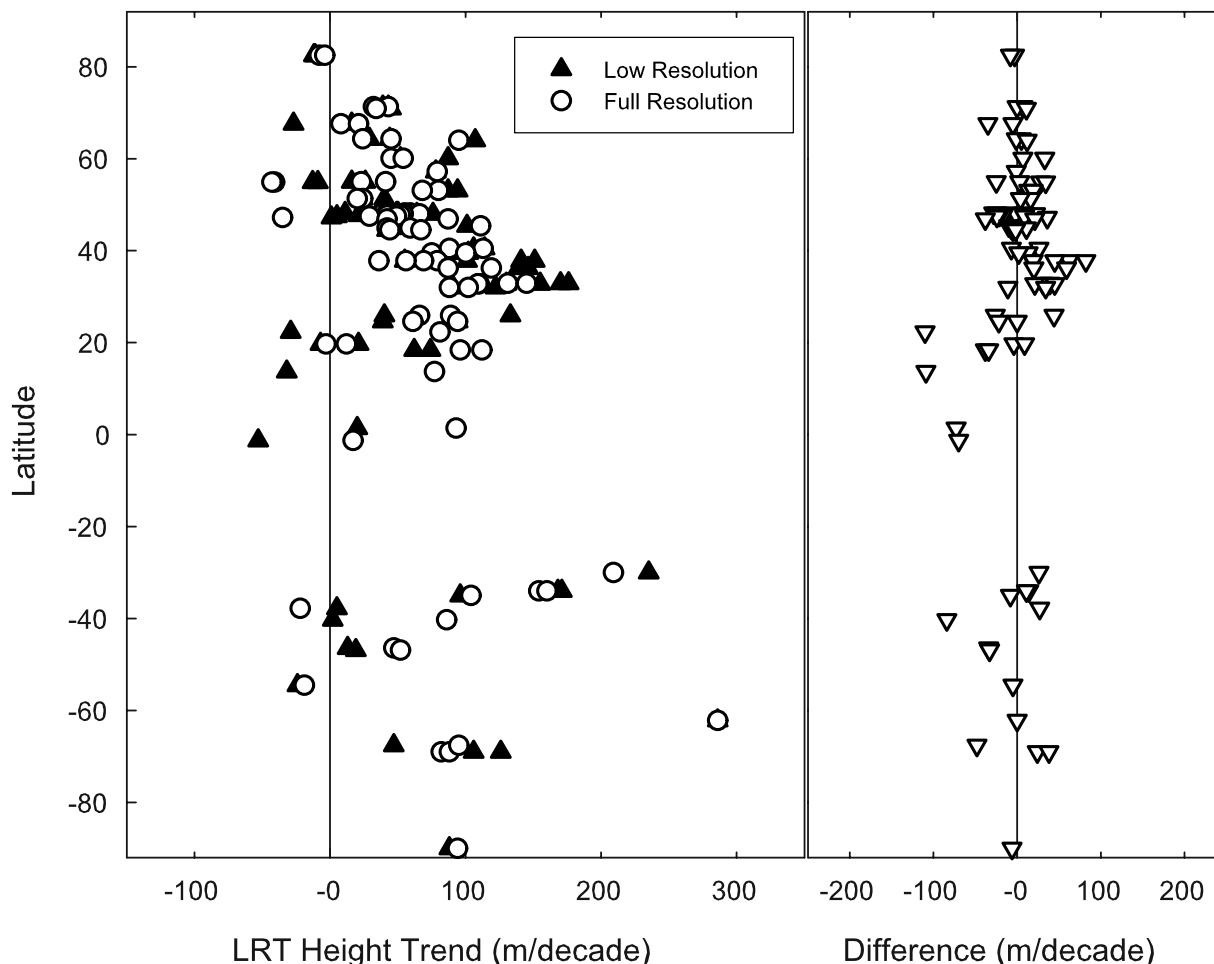


Figure A1. (left) Tropopause height trends (m/decade) for 1980–2004 as a function of latitude based on full resolution (open circles) and low-resolution (solid triangles) data. (right) Trend differences, low resolution minus full resolution.

[50] Tropopause height trends over 1980–2004 are upward at almost all of the stations analyzed, yielding a global trend of 64 ± 21 m/decade, a corresponding global LRT pressure trend of -1.7 ± 0.6 hPa/decade, and associated LRT temperature decrease of 0.41 ± 0.09 K/decade (or net changes of 160 m, -4.2 hPa and -1.0 K). These LRT trends are accompanied by significant stratospheric cooling and smaller tropospheric warming. However, the strength of the LRT trends is spatially correlated with that of the stratospheric temperature trend but there is no significant correlation between LRT trends and tropospheric temperature trends. Whether this result is physically meaningful or is a statistical artifact of the larger stratospheric than tropospheric trend signal is unclear.

[51] The sensitivity of tropopause height trends to stratospheric temperature trends is about 100 m/K, which is 20–30 times weaker than the corresponding sensitivity for synoptic or monthly timescales. A similar small value of 200 m/K is found for relating QBO variations in tropopause height and lower stratospheric temperature. This suggests that the coupling of tropopause height and stratospheric temperatures on interannual timescales involves different or additional mechanisms than for synoptic/monthly scales. Radiative effects are a likely contributor to this balance; the

relatively long radiative timescale in the lower stratosphere (~ 30 days) suggests that radiation is relatively unimportant for synoptic scales, but probably a large influence for inter-annual changes. We note that the radiosonde data analyzed here do not allow separation of this sensitivity between the tropics and extratropics (because there are few tropical stations and our results are based primarily on extratropics). Such a difference in sensitivity might be expected because the equilibrium structure and dynamical balance of the tropopause is fundamentally different between the tropics (radiative-convective balance [e.g., Thuburn and Craig, 2002]) versus extratropics (baroclinic wave dynamics [e.g., Haynes *et al.*, 2001; Schneider, 2004]).

[52] The observed correlation of tropopause height trends with stratospheric temperature trends, plus observation of a significant QBO signal in tropopause height time series, suggest that at these lowest frequencies the tropopause is primarily coupled with stratospheric temperatures. Conversely, tropopause height trends and tropospheric temperature trends are uncorrelated (although the smallness and uncertainties in the latter may influence this result). Therefore, as an indicator of climate change, long-term changes in the tropopause may carry less information about changes throughout the vertical temperature profile than has been

suggested by previous studies using reanalyses and global climate models.

Appendix A: Effect of Vertical Resolution of Sounding Data on Lapse Rate Tropopause Statistics

[53] Reanalysis data and climate model simulations have lower vertical resolution than radiosonde data, which could influence both the precision and accuracy of derived lapse rate tropopause heights. To investigate the effect of vertical resolution of temperature sounding data on LRT statistics, we repeated our analyses using radiosonde profiles degraded by elimination of all of the “significant” data levels. For each sounding, temperature and height data at the “mandatory” levels (1000, 850, 700, 500, 400, 300, 200, 150, 100, 50, 30, 20, 10, 7, 5, 3, 2, and 1 hPa) were used to evaluate lapse rates at intermediate levels (between pairs of adjacent mandatory levels), and the LRT was identified by interpolation (in height coordinates) of the lapse rate data to a level at which the LRT definition was satisfied. Using these LRT data, we computed all of the same climatological statistics as was done with the full resolution data.

[54] Climatological annual-average LRT height and pressure based on the low-resolution data (not shown) show the same overall patterns as obtained using the full resolution soundings (Figure 3). However, small biases were found, with LRT pressure and height differences ranging from -6 to 9 hPa and -164 to 364 m, respectively, with mean absolute differences of 2.7 hPa and 96 m.

[55] Trends in LRT height for the period 1980–2004 evaluated from the low- and full resolution data are shown in Figure A1 (left). At some stations the values are very similar, but at many the differences (Figure A1, right) are similar in magnitude to the trends themselves. The range of trend differences (low minus full resolution) is -110 to 82 m/decade, the mean absolute difference is 24 m/decade, and typical differences are 10 – 50% of the trend based on the full resolution data. There is better agreement for large-scale average trends. Zonal trends from the full resolution data (Figure 10a) are not statistically significantly different from those based on the low-resolution data (not shown). The global LRT height trend from low-resolution data is 51 ± 26 m/decade, compared with 64 ± 21 m/decade for full resolution, and comparable values for LRT pressure trends are -2.1 ± 0.7 and -1.7 ± 0.6 hPa/decade.

[56] On the basis of this analysis, we conclude that climatological statistics based on lower-resolution data contain biases that vary from location to location and that local trend estimate from lower-resolution data can be biased with respect to those based on full resolution data, but the biases in global-average trends are less severe.

[57] **Acknowledgments.** We thank Fei Wu (NCAR) for data processing assistance and Melissa Free and Val Garcia (NOAA), Ben Santer (LLNL), and two anonymous reviewers for helpful suggestions. This work is partially supported by the NASA ACMAP program. The National Center for Atmospheric Research is sponsored by the National Science Foundation.

References

- Angell, J. K., and J. Korshover (1964), Quasi-biennial variations in temperature, total ozone and tropopause height, *J. Atmos. Sci.*, *21*, 479–492.
- Añel, J. A., L. Gimeno, L. de la Torre, and R. Nieto (2006), Changes in tropopause height for the Eurasian region determined from CARDS radiosonde data, *Naturwissenschaften*, doi:10.1007/S00114-006-0147-5.
- Chakrabarty, D. K., N. C. Shah, K. V. Pandya, and S. K. Peshin (2000), Long-term trend of tropopause over New Delhi and Thiruvananthapuram, *Geophys. Res. Lett.*, *27*(15), 2181–2184.
- Durre, I., R. S. Vose, and D. B. Wuertz (2006), Overview of the Integrated Global Radiosonde Archive, *J. Clim.*, *19*, 53–68, doi:10.1175/JCLI3594.1.
- Elliott, W. P., R. J. Ross, and W. H. Blackmore (2002), Recent changes in NWS upper-air observations with emphasis on changes from VIZ to Vaisala radiosondes, *Bull. Am. Meteorol. Soc.*, *83*, 1003–1017.
- Forster, P. M. de F., and K. Tourpali (2001), Effect of tropopause height changes on the calculation of ozone trends and their radiative forcing, *J. Geophys. Res.*, *106*, 12,241–12,252.
- Free, M., D. J. Seidel, J. K. Angell, J. Lanzante, I. Durre, and T. C. Peterson (2005), Radiosonde Atmospheric Temperature Products for Assessing Climate (RATPAC): A new data set of large-area anomaly time series, *J. Geophys. Res.*, *110*, D22101, doi:10.1029/2005JD006169.
- Gaffen, D. J. (1993), Historical changes in radiosonde instruments and practices, *WMO/TD 541, Instrum. Obs. Methods Rep. 50*, 123 pp., World Meteorol. Organ., Geneva.
- Gaffen, D. J. (1994), Temporal inhomogeneities in radiosonde temperature records, *J. Geophys. Res.*, *99*, 3667–3676.
- Gettelman, A., W. J. Randel, S. Massie, F. Wu, W. G. Read, and J. M. Russell (2001), El Niño as a natural experiment for studying the tropical tropopause region, *J. Clim.*, *14*, 3375–3392.
- Haynes, P., J. Scinocca, and M. Greenslade (2001), Formation and maintenance of the extratropical tropopause by baroclinic eddies, *Geophys. Res. Lett.*, *28*(22), 4179–4182.
- Highwood, E. J., B. J. Hoskins, and P. Berrisford (2000), Properties of the Arctic tropopause, *Q. J. R. Meteorol. Soc.*, *126*, 1515–1532.
- Hoinka, K. P. (1998), Statistics of the global tropopause pressure, *Mon. Weather Rev.*, *126*, 3303–3325.
- Hoinka, K. P. (1999), Temperature, humidity, and wind at the global tropopause, *Mon. Weather Rev.*, *127*, 2248–2265.
- Hoskins, B. J., M. E. McIntyre, and A. W. Robertson (1985), On the use and significance of isentropic potential vorticity maps, *Q. J. R. Meteorol. Soc.*, *111*, 877–946.
- Kiladis, G. N., K. H. Straub, G. C. Reid, and K. S. Gage (2001), Aspects of interannual and intraseasonal variability of the tropopause and lower stratosphere, *Q. J. R. Meteorol. Soc.*, *127*, 1961–1984.
- Lanzante, J. R., S. A. Klein, and D. J. Seidel (2003), Temporal homogenization of monthly radiosonde temperature data. Part I: Methodology, *J. Clim.*, *16*, 224–240.
- Makhover, Z. M. (1979), Features of the tropopause distribution over the globe (in Russian), *Meteorol. Geophys.*, *12*, 33–39.
- Nagurny, A. P. (1998), Climatic characteristics of the tropopause over the Arctic Basin, *Ann. Geophys.*, *16*, 110–115.
- Naujokat, B. (1986), An update of the observed quasi-biennial oscillation of stratospheric winds over the tropics, *J. Atmos. Sci.*, *43*, 1873–1877.
- Parker, D. E., and D. I. Cox (1995), Towards a consistent global climatological rawinsonde data-base, *Int. J. Climatol.*, *15*, 473–496.
- Randel, W. J., and F. Wu (2006), Biases in stratospheric and tropospheric temperature trends derived from historical radiosonde data, *J. Clim.*, *19*, 2094–2104.
- Randel, W. J., F. Wu, R. Swinbank, J. Nash, and A. O’Neill (1999), Global QBO circulation derived from UKMO stratospheric analyses, *J. Atmos. Sci.*, *56*, 457–474.
- Randel, W. J., F. Wu, and D. J. Gaffen (2000), Interannual variability of the tropical tropopause derived from radiosonde data and NCEP reanalyses, *J. Geophys. Res.*, *105*, 15,509–15,524.
- Redder, C. R., J. K. Luers, and R. E. Eskridge (2004), Unexplained discontinuity in the U.S. radiosonde temperature data. Part II: Stratosphere, *J. Atmos. Oceanic Technol.*, *21*, 1133–1144.
- Reid, G. C., and K. S. Gage (1985), Interannual variations in the height of the tropical tropopause, *J. Geophys. Res.*, *90*, 5629–5635.
- Santer, B. D., T. M. L. Wigley, J. S. Boyle, D. J. Gaffen, J. J. Hnilo, D. Nychka, D. E. Parker, and K. E. Taylor (2000), Statistical significance of trend differences in layer-average temperature time series, *J. Geophys. Res.*, *105*, 7337–7356.
- Santer, B. D., et al. (2003a), Behavior of tropopause height and atmospheric temperature in models, reanalyses, and observations: Decadal changes, *J. Geophys. Res.*, *108*(D1), 4002, doi:10.1029/2002JD002258.
- Santer, B. D., et al. (2003b), Contributions of anthropogenic and natural forcing to recent tropopause height changes, *Science*, *301*, 479–483.
- Santer, B. D., et al. (2004), Identification of anthropogenic climate change using a second-generation reanalysis, *J. Geophys. Res.*, *109*, D21104, doi:10.1029/2004JD005075.

- Sausen, R., and B. D. Santer (2003), Use of changes in tropopause height to detect human influences on climate, *Meteorol. Z.*, *12*, 131–136.
- Schneider, T. (2004), The tropopause and the thermal stratification in the extratropics of a dry atmosphere, *J. Atmos. Sci.*, *61*, 1317–1340.
- Seidel, D. J., R. J. Ross, J. K. Angell, and G. C. Reid (2001), Climatological characteristics of the tropical tropopause as revealed by radiosondes, *J. Geophys. Res.*, *106*, 7857–7878.
- Shepherd, T. G. (2002), Issues in stratosphere-troposphere coupling, *J. Meteorol. Soc. Jpn.*, *80*, 769–792.
- Sherwood, S. C., J. R. Lanzante, and C. L. Meyer (2005), Radiosonde daytime biases and late 20th century warming, *Science*, *309*, 1556–1559.
- Steinbrecht, W., H. Claude, U. Kohler, and K. P. Hoinka (1998), Correlations between tropopause height and total ozone: Implications for long-term changes, *J. Geophys. Res.*, *103*, 19,183–19,192.
- Thompson, D. W. J., J. M. Wallace, and G. C. Hegerl (2000), Annular modes in the extratropical circulation. Part II: Trends, *J. Clim.*, *13*, 1018–1036.
- Thorne, P. W., D. E. Parker, S. F. B. Tett, P. D. Jones, M. McCarthy, H. Coleman, and P. Brohan (2005), Revisiting radiosonde upper-air temperatures from 1958 to 2002, *J. Geophys. Res.*, *110*, D18105, doi:10.1029/2004JD005753.
- Thuburn, J., and G. C. Craig (2002), On the temperature structure of the tropical stratosphere, *J. Geophys. Res.*, *107*(D2), 4017, doi:10.1029/2001JD000448.
- Varotsos, C., C. Cartalis, A. Vlamakis, C. Tzanis, and I. Keramitsoglou (2004), The long-term coupling between column ozone and tropopause properties, *J. Clim.*, *17*, 3843–3854.
- Wolter, K., and M. S. Timlin (1998), Measuring the strength of ENSO: How does 1997/98 rank?, *Weather*, *53*, 315–324.
- Wong, S., and W.-C. Wang (2000), Interhemispheric asymmetry in the seasonal variation of the zonal mean tropopause, *J. Geophys. Res.*, *105*, 26,645–26,659.
- World Meteorological Organization (1957), Meteorology—A three-dimensional science: Second session of the Commission for Aerology, *WMO Bull. IV*, no. 4, pp. 134–138, Geneva.
- Zängl, G., and K. P. Hoinka (2001), The tropopause in the polar regions, *J. Clim.*, *14*, 3117–3139.

W. J. Randel, National Center for Atmospheric Research, P. O. Box 3000, Boulder, CO 80307-3000, USA.

D. J. Seidel, NOAA Air Resources Laboratory (R/ARL), 1315 East West Highway, Silver Spring, MD 20910, USA. (dian.seidel@noaa.gov)